Supplemental Material: Energy-Efficient Localized Routing in Random Multihop Wireless Networks

Yu Wang* Xiang-Yang Li‡ Wen-Zhan Song† Minsu Huang* Teresa A. Dahlberg*

I. Detailed Theoretical Proofs

In this section, we provide the detailed proofs of Lemma 2, Theorem 5, and Theorem 6.

A. *Proof of Lemma 2*

Lemma 2 *We have $\angle wut \leq \alpha$ if $\|uv\|+\|vw\| \leq r$, $\angle vut \leq \alpha$ and $\angle wvt \leq \alpha$.*

Proof: Without loss of generality, we assume that node v is on top of the line crossing u and t. Let $\lhd xuy$ and $\lhd avb$ be the sectors of the forwarding region defined by node u and v respectively for destination node t. To prove the lemma, it is equivalent to show that the intersected region by $\lhd avb$ with disk $\mathbf{D}(u, r)$ is inside the sector $\lhd xuy$. See Figure 1 for illustration. When node v is on top of line ut, it is easy to show that segment va will intersect the arc xy of sector $\lhd xuy$, and we use p to denote such intersection. We then prove the lemma based on two separate cases whether point y is inside the disk $\mathbf{D}(v, r)$ or not.

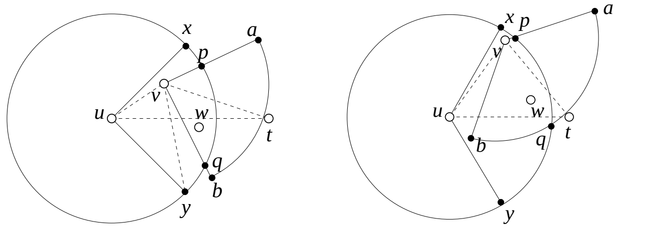

(a) vb intersecting $\mathbf{D}(u, r)$ (b) vb not intersecting $\mathbf{D}(u, r)$

Fig. 1. Illustrations of possible short cut: $\angle wut \leq \alpha$.

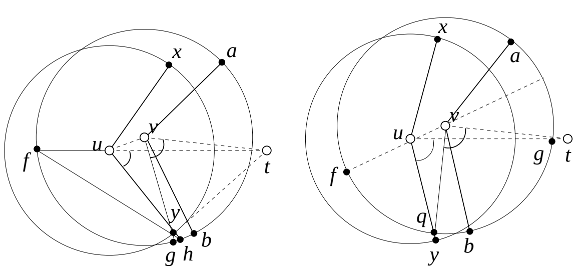

(a) y inside $\mathbf{D}(v, r)$ (b) y outside $\mathbf{D}(v, r)$

Fig. 2. Proof that $\lhd avb \cap \mathbf{D}(u, r)$ is contained inside $\lhd xuy$.

1) We first consider the subcase when y is inside $\mathbf{D}(v, r)$. See Figure 2 (a) for illustration. Let h be the intersecting point of ray uy with disk $\mathbf{D}(v, r)$. Let point f be the intersecting point of disk $\mathbf{D}(v, r)$ with line ut that is inside disk $\mathbf{D}(u, r)$. Then obviously, $\|fh\| > \|uh\| > \|uy\| = r > \|uf\|$. Thus, $\angle fhu < \angle ufh$ and $\angle fhu + \angle ufh = \angle tuh = \alpha$. It implies that $\alpha < 2\angle hfu = 2\angle hft$. In addition, clearly, we have $\angle yvt > \angle hvt = 2\angle hft > \alpha$. Thus, point b must be on the arc ga, where point g is the intersecting point of ray vy with disk $\mathbf{D}(v, r)$. This implies that segment vb will intersect the arc xy of disk $\mathbf{D}(u, r)$. Thus, $\lhd avb \cap \mathbf{D}(u, r)$ is contained insider the forwarding region $\lhd xuy$.
2) We then consider the subcase when y is not inside $\mathbf{D}(v, r)$. See Figure 2 (b) for illustration. Let point g be the intersecting point of segment ut with disk $\mathbf{D}(v, r)$. Let q be the intersecting point of segment uy with $\mathbf{D}(v, r)$. It is easy to show that $\angle gvq > \angle guq = \alpha$ since v is the circumcenter and points g and y are on the same half circle cut by diameter passing uv. Thus, $\angle tvq > \angle gvq > \alpha$. It implies that point b must be on the arc qa. It is then straightforward to show that $\lhd avb \cap \mathbf{D}(u, r)$ is contained insider the forwarding region $\lhd xuy$.

Since $\|uw\| \leq \|uv\| + \|vw\| < r$, node w is inside $\mathbf{D}(u, r)$. Since w is inside $\lhd avb$, thus w belongs to $\lhd avb \cap \mathbf{D}(u, r)$, which is contained inside the forwarding sector $\lhd xuy$ of node u. Consequently, $\angle wut \leq \alpha$. This completes the proof. ■

B. *Proof of Theorem 5*

Theorem 5 The LEARN routing (with parameter $\alpha < \frac{\pi}{3}$) will find a path from the source to the target *asymptotically almost surely* when the transmission radius r satisfies $n\pi r^2 = \beta \ln n$ for any constant $\beta > \beta_0 = \frac{\pi}{\alpha}$.

Proof: To prove this, it is sufficient to show that when each node has a transmission radius r satisfying the above condition, for every node u and every node v there is always a node $w \in \mathcal{P}_n$ such that $\angle wuv \leq \alpha$ and $\|w - u\| \leq r$, *i.e.*, any intermediate node u can find a "better" neighbor w towards the destination node v.

Given a point distribution $\mathcal{P}_n$, let $\mathcal{S}(\mathcal{P}_n, r)$ be the minimum number of such neighboring nodes w that can be chosen by any intermediate node u for any possible destination v. As proved in [1], it suffices to prove that the cardinality $|\mathcal{S}(\mathcal{P}_n, r)| > 0$. We actually will show a much stronger result that $\mathcal{S}(\mathcal{P}_n, r) \geq \frac{1}{2}\mathcal{L}(\frac{\beta}{\beta_2}) \ln n$ for any constant $\beta_0 < \beta_2 < \beta$. Here $\mathcal{L}(x)$ is defined in [1] as $\mathcal{L}(x) = x\phi^{-1}(1/x)$ for $x > 0$ and $\phi(x) = 1 + x \ln x - x$ for $x > 0$.

* Y. Wang, M. Huang and T. Dahlberg are with Department of Computer Science, University of North Carolina at Charlotte, Charlotte, NC, USA.

‡ X.-Y. Li is with Tsinghua National Laboratory for Information Science and Technology, Tsinghua University, Beijing, China, and Department of Computer Science, Illinois Institute of Technology, Chicago, IL, USA.

† W.-Z. Song is with Department of Computer Science, Georgia State University, Atlanta, GA, USA.

Notice that, given a node u, the area that node u can choose its neighbor to forward data for a given destination t is a sector of disk $\mathbf{D}(u,r)$ with angle 2α. Here $\mathbf{D}(u,r)$ denotes the disk centered at node u with radius r. We use $\mathbf{Y}$ to denote such sector. Let d denote the diameter of this sector $\mathbf{Y}$. Clearly $d=r$ when $\alpha \le \frac{\pi}{6}$, and $d = 2\sin\alpha \cdot r$ when $\frac{\pi}{6} \le \alpha < \frac{\pi}{3}$.

Assume that the space is partitioned into grids (quadrates) of side length η, which we call it η-tessellation of space. Here, we consider an ϵd-tessellation, where ϵ is a constant to be specified later. A *polyquadrate* is defined as the set of quadrates that intersect with a convex and compact region, *e.g.*, $\mathbf{Y}$. Notice that when the grid-partition shifts, we will have different polyquadrates for the fixed region $\mathbf{Y}$. A polyquadrate in a η-tessellation is said to have a *span* s if it can be contained in a square of side-length $s \cdot \eta$. We are only interested in polyquadrates that has span at most $\frac{1}{\epsilon}$ and area at least a certain fraction of πr^2. Assume that, given $\mathbf{Y}$, there are I_n different such polyquadrates that are completely contained inside, with span at most $\frac{1}{\epsilon}$ and area at least $\delta_1 \pi r^2$. Here δ_1 is a constant to be specified later. For ith such polyquadrate, let X_i denote the number of nodes of V contained inside. Also assume that there are I'_n different such polyquadrates that intersect the boundary of $\mathbf{Y}$ with span at most $\frac{1}{\epsilon}$ and area at least $\delta_2 \pi r^2$. Here δ_2 is a constant to be specified later. For ith such polyquadrate, let X'_i denote the number of nodes of V contained inside. According to Lemma 4 of [1], we have

$$\begin{aligned} I_n &= O\left(\left(\frac{1}{\epsilon d}\right)^2\right) = O\left(\frac{n}{\ln n}\right), \\ I'_n &= O\left(\frac{1}{\epsilon d}\right) = O\left(\sqrt{\frac{n}{\ln n}}\right). \end{aligned}$$

Furthermore, X_i are Poisson random variables with rate at least $\delta_1 \pi r^2 \cdot n = \beta\delta_1 \ln n$. Similarly, X'_i are Poisson random variables with rate at least $\delta_2 \pi r^2 \cdot n = \beta\delta_2 \ln n$. Then according to Lemma 6 of [1], we have $\min_{i=1}^{I_n} X_i > \mathcal{L}(\beta')\ln n$ *a.a.s.* for any $1<\beta'<\delta_1\beta$, and $\min_{i=1}^{I'_n} X'_i > \frac{1}{2}\mathcal{L}(2\beta'')\ln n$ *a.a.s.* for any $1<\beta''<\delta_2\beta$. Thus, we have *a.a.s.*

$$\min(\min_{i=1}^{I_n} X_i, \min_{i=1}^{I'_n} X'_i) \ge \min(\mathcal{L}(\beta'), \frac{1}{2}\mathcal{L}(2\beta''))\ln n$$

for any $1<\beta'<\delta_1\beta$, and $1<\beta''<\delta_2\beta$.

To prove the theorem, it is sufficient to show that

$$\mathcal{S}(\mathcal{P}_n, r) \ge \min(\min_{i=1}^{I_n} X_i, \min_{i=1}^{I'_n} X'_i).$$

In other words, we only need to show that for any $\mathbf{Y}$, it

1) either contains a polyquadrate P has span at most $\frac{1}{\epsilon}$ and area at least $\delta_1 \pi r^2$ when $\mathbf{Y}$ is inside Ω;
2) or contains a polyquadrate P' has span at most $\frac{1}{\epsilon}$ and area at least $\delta_1 \pi r^2$ when $\mathbf{Y}$ intersects boundary of Ω.

First consider the case when $\mathbf{Y}$ is contained inside Ω. For the polyquadrate P, we consider the induced polyquadrate (denoted by $P_{-\sqrt{2}\epsilon d}$, formed by all quadrates of P that intersect with region $\mathbf{Y}_{-\sqrt{2}\epsilon d}$. Here $\mathbf{Y}_{-x}$ denotes the region of $\mathbf{Y}$ that are of distance at least x from the boundary of $\mathbf{Y}$. The span of polyquadrate $P_{-\sqrt{2}\epsilon d}$ is at most $\lceil \frac{d-2\sqrt{2}\epsilon d}{\epsilon d} \rceil + 1 < \frac{1}{\epsilon}$. The area of the polyquadrate $P_{-\sqrt{2}\epsilon d}$ is at least the area of $\mathbf{Y}_{-\sqrt{2}\epsilon d}$. Notice that $|\mathbf{Y}_{-\sqrt{2}\epsilon d}| = \alpha(r - 2\sqrt{2}\epsilon d)^2$. Thus, it is sufficient to require that

$$|\mathbf{Y}_{-\sqrt{2}\epsilon d}| = \alpha(r - 2\sqrt{2}\epsilon d)^2 \ge \delta_1 \pi r^2.$$

We then consider the case that $\mathbf{Y}$ intersects the boundary of Ω. Then let $\mathbf{Y}'$ be the part that are fully contained inside Ω. Similarly, we consider the polyquadrate $P'_{-\sqrt{2}\epsilon d}$ induced by $\mathbf{Y}'_{-\sqrt{2}\epsilon d}$, *i.e.*, the quadrates that are contained inside Ω and $\mathbf{Y}$. Clearly, the span of this polyquadrate is also at most $\frac{1}{\epsilon}$. It is not difficult to show that the area of $\mathbf{Y}'$ is at least $\frac{1}{2}$ of the area of $\mathbf{Y}$. Thus, the area $|P'_{-\sqrt{2}\epsilon d}|$ of polyquadrate $P'_{-\sqrt{2}\epsilon d}$ is at least $|P'_{-\sqrt{2}\epsilon d}| \ge |\mathbf{Y}'_{-\sqrt{2}\epsilon d}| \ge \frac{1}{2}|\mathbf{Y}_{-\sqrt{2}\epsilon d}|$. Thus, it is sufficient to require that

$$\frac{1}{2}|\mathbf{Y}_{-\sqrt{2}\epsilon d}| = \frac{1}{2}\alpha(r - 2\sqrt{2}\epsilon d)^2 \ge \delta_2 \pi r^2.$$

In summary, we require the following conditions about the parameters δ_1, δ_2, ϵ:

$$\begin{cases} \beta\delta_1 > 1, & \alpha(1 - 2\sqrt{2}\epsilon\frac{d}{r})^2 \ge \delta_1\pi, \\ \beta\delta_2 > 1, & \alpha(1 - 2\sqrt{2}\epsilon\frac{d}{r})^2 \ge 2\delta_2\pi. \end{cases}$$

Clearly, we can choose $\delta_2 = \frac{1}{2}\delta_1$. Notice that we defined $\beta_0 = \frac{\pi}{\alpha}$. Thus, it is equivalent to require that

$$\begin{cases} \beta\delta_1 > 1, \\ (1 - 2\sqrt{2}\epsilon\frac{d}{r})^2 \ge \delta_1\beta_0. \end{cases}$$

This has a solution when $\beta > \beta_0$. For example, we can select a constant β_1 such that $\beta_0 < \beta_1 < \beta$ and let $\delta_1 = \frac{1}{\beta_1}$. Then $\epsilon = \frac{1-\sqrt{\beta_0/\beta_1}}{2\sqrt{2}d_0}$. Here $d_0 = \frac{d}{r}$, which is 1 when $\alpha \le \frac{\pi}{6}$ and is $2\sin\alpha$ when $\frac{\pi}{6} \le \alpha < \frac{\pi}{3}$. In this case, we can choose β_2 such that $\beta_0 < \beta_1 < \beta_2 < \beta$ and set $\beta' = \frac{\beta}{\beta_2}$ and $\beta'' = \beta'/2$. Then we have

$$\mathcal{S}(\mathcal{P}_n, r) \ge \frac{1}{2}\mathcal{L}(\frac{\beta}{\beta_2})\ln n.$$

Notice that when $r = \sqrt{\frac{\beta \ln n}{\pi n}}$ for some $\beta > \beta_0 = \frac{\pi}{\alpha}$, the probability that an intermediate node u cannot find a forwarding node w to a destination t is $e^{-n\alpha r^2}$, *i.e.*, the probability that the sector does not contain any node. Since the path from any source node to any destination node contains at most n hops, the probability that LEARN routing protocol is successful is at least $(1 - e^{-n\alpha r^2})^n = (1 - n^{-\frac{\beta}{\beta_0}})^n > 1 - \frac{1}{n^{\beta/\beta_0 - 1}}$, which goes to 1 as $n \to \infty$. This completes our proof. ■

C. Proof of Theorem 6

Theorem 6 The LEARN routing (with parameter $\alpha < \frac{\pi}{3}$) will *not* be able to find a path from the source to the target *asymptotically almost surely* when the transmission radius r satisfies $n\pi r^2 = \beta \ln n$ for any constant $\beta < \beta_0 = \frac{\pi}{\alpha}$.

Proof: We basically will show that, *a.a.s.*, there are two nodes u and v such that we cannot find a node w for forwarding by node u, *i.e.*, there does not exist node w with $\angle wuv \le \alpha$ and $\|w - u\| \le r$. Recall that $r = \sqrt{\frac{\beta \ln n}{\pi n}}$ for $\beta < \beta_0$. Again we partition the space using grids, where each grid has side-length ηr for a constant $0 < \eta$ to be specified later. Then it is easy to show that the number of cells, denoted by I_n here, that are fully contained inside the compact and convex region Ω with unit area is $\Theta(\frac{1}{\eta^2 r^2}) = \Theta(\frac{n}{\ln n})$. Let $E_{u,v}$ denote the event that no forwarding node w (with $\angle wuv \leq \alpha$ and $\|w-u\| \leq r$) exists for node u to reach node v. Then to prove our theorem, it is equivalent to prove that the probability at least one of the event $E_{u,v}$ happens asymptotically almost surely, *i.e.*, $1 - \mathbf{Pr}(\text{none of event } E_{u,v} \text{ happens}) > 0$. Clearly, the events $E_{u,v}$ are not independent for all pairs u and v. We will consider a special subset of events that are independent. Consider any cell produced by the grid partition that are contained inside Ω. See Figure 3 (a) for an illustration. For each cell, we draw a shaded square with side-length $(\eta - 2(1+\delta))r$ and it is of distance $(1+\delta)r$ to the boundary of the cell. We only consider the case when node u is located in the shaded square as in Figure 3 (a). We also restrict the node v to satisfy that $r < \|u-v\| \leq (1+\delta)r$, *i.e.*, in the torus area in Figure 3 (b). Clearly, node v will also be inside this cell, and the shaded sector area (see Figure 3 (b)) where the possible forwarding node could locate is also inside this cell. Thus, events E_{u_1,v_1} and E_{u_2,v_2} will be independent if u_1 and u_2 are selected as above from different cells.

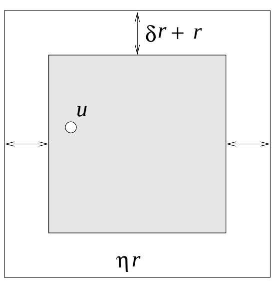

(a) selection of u

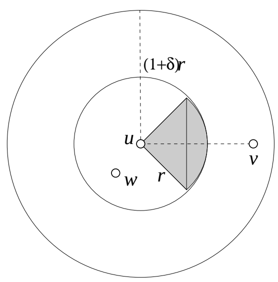

(b) no forwarding node

Fig. 3. Illustrations of the proof of lower bound: (a) a cell and the area where we will select a node u, (b) the event that node u cannot find a forwarding node w to reach a node v.

Then for each cell i, we compute the probability that the event E_{u_i,v_i} happens, where u_i is selected from the shaded square of cell i and v_i is selected such that $r < \|v_i - u_i\| \leq (1+\delta)r$. Recall that for any region with area A, the probability that this region is empty of any nodes (for Poisson process with rate n) is e^{-nA}. Clearly, the probability that node u_i exists is $1 - e^{-n(\eta-2-2\delta)^2 r^2}$ since the shared square has area $(\eta-2-2\delta)^2 r^2$; the probability that node v_i exists is $1 - e^{-n\pi(\delta^2+2\delta)r^2}$ since the torus has area $\pi(\delta^2+2\delta)r^2$. Given node u_i and v_i, the probability that event E_{u_i,v_i} happens is $e^{-n\alpha r^2} = e^{-\beta/\beta_0 \ln n} = n^{-\beta/\beta_0}$. Consequently, event E_{u_i,v_i} happens for some node pairs u and v is

$$\begin{aligned} & \mathbf{Pr}(E_{u_i,v_i}) \\ \geq \; & (1 - e^{-n(\eta-2-2\delta)^2 r^2})(1 - e^{-n\pi(\delta^2+2\delta)r^2})n^{-\beta/\beta_0} \\ = \; & (1 - n^{-\beta(\eta-2-2\delta)^2/\pi})(1 - n^{-\beta(\delta^2+2\delta)})n^{-\beta/\beta_0}. \end{aligned}$$

Thus, the probability that the LEARN routing fails to find a path for some pair of source and destination nodes is

$$\begin{aligned} & \mathbf{Pr}(\text{at least one of events } E_{u,v} \text{ happens}) \\ \geq \; & \mathbf{Pr}(\text{at least one of events } E_{u_i,v_i} \text{ happens}) \\ = \; & 1 - \mathbf{Pr}(\text{none of event } E_{u_i,v_i} \text{ happens}) \\ = \; & 1 - (1 - \mathbf{Pr}(E_{u_i,v_i}))^{I_n} \\ = \; & 1 - e^{I_n \cdot \ln(1 - \mathbf{Pr}(E_{u_i,v_i}))} \\ \geq \; & 1 - e^{-I_n \cdot \mathbf{Pr}(E_{u_i,v_i})}. \end{aligned}$$

Notice that $I_n \cdot \mathbf{Pr}(E_{u_i,v_i}) = \Theta(\frac{n}{\ln n})(1 - n^{-\beta(\eta-2-2\delta)^2/\pi})(1 - n^{-\beta(\delta^2+2\delta)})n^{-\beta/\beta_0} \simeq \frac{n^{1-\beta/\beta_0}}{\ln n}$, which goes to ∞ as $n \to \infty$ when $\beta < \beta_0$, $\eta - 2 - 2\delta > 0$, and $\delta > 0$. This can be easily satisfied, *e.g.*, $\delta = 1$, $\eta = 5$. Thus, $\lim_{n\to\infty} 1 - e^{-I_n \cdot \mathbf{Pr}(E_{u_i,v_i})} = 1$. This completes the proof. ■

II. Performance Evaluation

In this section, we provide the simulation results on the performance of our LEARN routing in random networks.

A. Critical Transmission Radius for LEARN Routing

We first study the study the critical transmission radius for proposed LEARN routing in random networks. In our experiments, we randomly distribute n wireless nodes in a 100×100 square region. Node density n is 50, 100, 200, 300, 400, and 500. The parameter α is $\pi/4$ or $\pi/6$. For each choice of α and n, 1000 networks are generated, and the critical transmission radius $\rho(V)$ is generated for each network V using Equation (1) in Section V.B. Figure 4 shows the histograms of the distribution of the critical transmission radius $\rho(V)$ in random networks with different size when $\alpha = \pi/4$.

Figure 5(a) and Figure 5(b) show the probability distribution functions of $\rho(V)$ of our LEARN routing when $\alpha = \pi/6$ and $\alpha = \pi/4$ respectively. It is clear that the CTR satisfies a transition phenomena, *i.e.*, there is a radius $\rho(V)$ such that LEARN routing can successfully deliver all packets when $r > \rho(V)$ and can not deliver some packets when $r < \rho(V)$. Notice that the transition becomes faster when the number of nodes increases. This confirms our theoretical analysis on the existence of CTR. In addition, from the figures, we can find that larger node density always leads to smaller value of CTR. The practical value of $\rho(V)$ is larger than the theoretical bound in our analysis, since the theoretical bound is standing for $n \to \infty$. However, the practical value will approach the theoretical bound with the increasing of n. When $n = 500$, it already becomes very near the theoretical bound. Compared the two cases with $\alpha = \pi/6$ and $\pi/4$, larger CTR is required if smaller restricted region (*i.e.* smaller α) is applied.

We also conduct simulations for 3D LEARN routing in 3D random networks. All parameters are same with the 2D case, except for the region now is a $100 \times 100 \times 100$ cubic region. Figure 5(c) and Figure 5(d) show the probability distribution functions of $\rho(V)$ of our 3D LEARN routing. The conclusions from these results are consistent with those from the 2D case. Notice that with the same amount of nodes, 3D network needs larger transmission radius to guarantee the delivery.

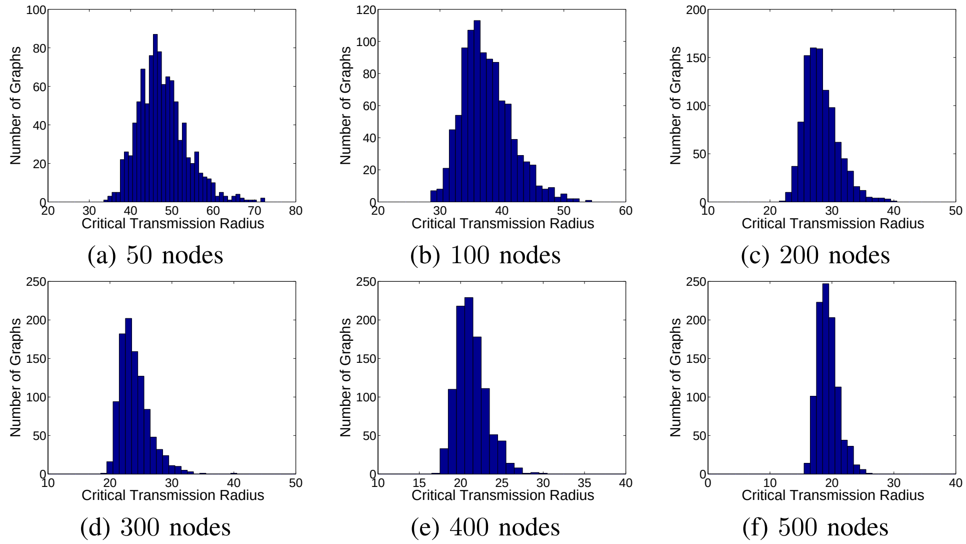

(a) 50 nodes (b) 100 nodes (c) 200 nodes

(d) 300 nodes (e) 400 nodes (f) 500 nodes

Fig. 4. The distributions of the critical transmission radius for LEARN routing in random networks when $\alpha = \pi/6$.

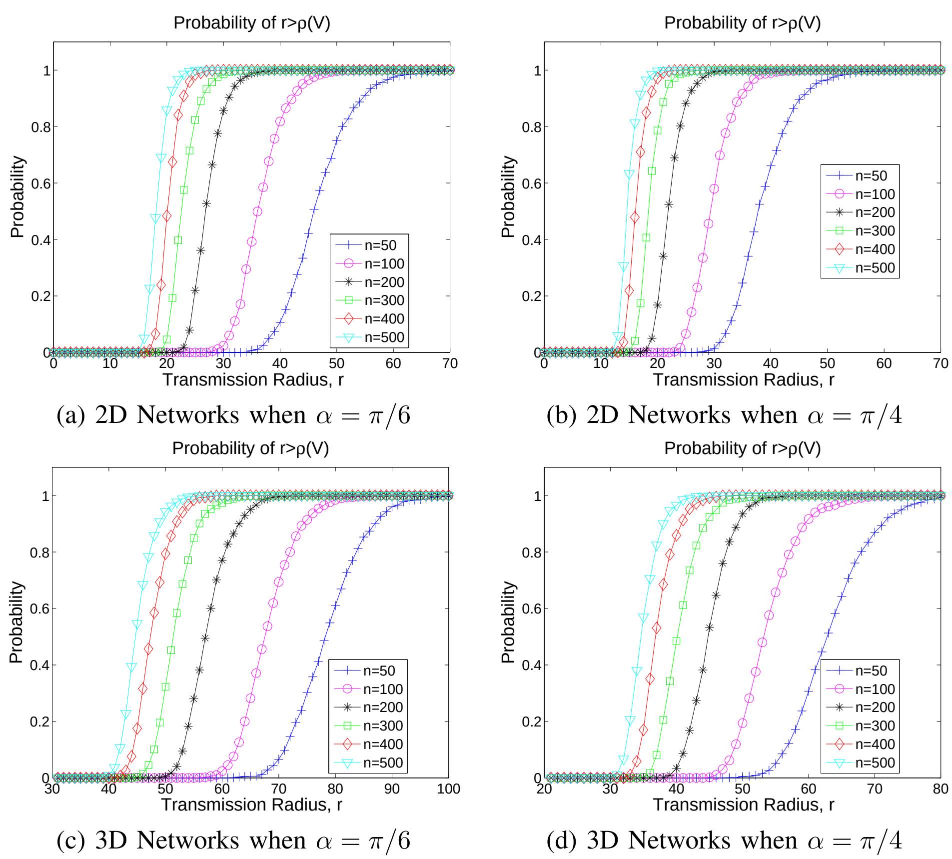

(a) 2D Networks when $\alpha = \pi/6$ (b) 2D Networks when $\alpha = \pi/4$

(c) 3D Networks when $\alpha = \pi/6$ (d) 3D Networks when $\alpha = \pi/4$

Fig. 5. The probability distributions of the critical transmission radius for LEARN routing in 2D/3D random networks when $\alpha = \pi/6$ or $\pi/4$.

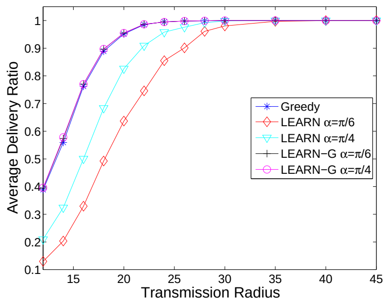

(a) Delivery Ratio

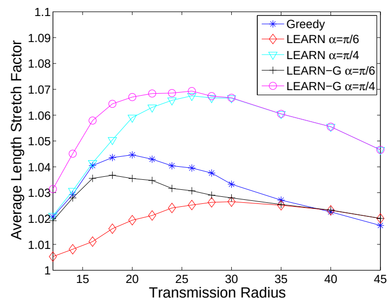

(b) Length Stretch Factor

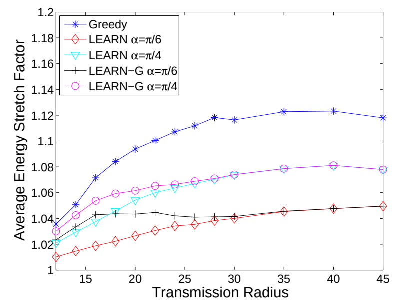

(c) Energy Stretch Factor

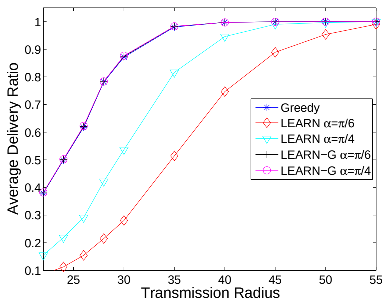

(d) Delivery Ratio

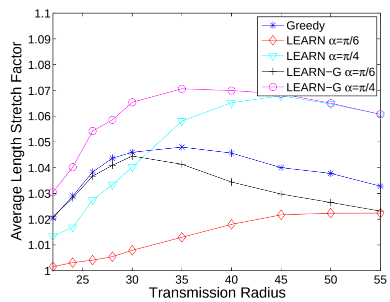

(e) Length Stretch Factor

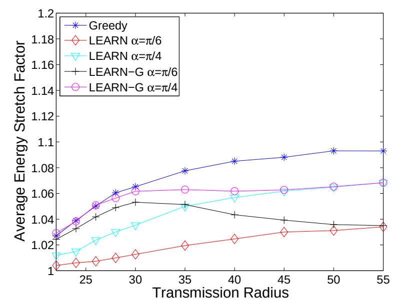

(f) Energy Stretch Factor

Fig. 6. Routing Performance of LEARN: Delivery ratio and path efficiency (length stretch factor and energy stretch factor) of different localized routing methods in random 2D/3D networks. The upper row is for 2D networks, while the lower row is for 3D networks.

B. Network Performance Comparisons

We implement the proposed LEARN routing in our simulator. By setting various transmission radii, we generate 100 connected random networks with 100 wireless nodes again in either a 100×100 rectangle region or a $100 \times 100 \times 100$ cubic region. We randomly select 100 source-destination pairs for each network and test both the classical greedy routing (Greedy) or variations of our proposed LEARN routing methods (specifically, LEARN or LEARN-G with $\alpha = \pi/6$ or $\pi/4$). All results presented hereafter are average values over all routes and networks. For energy model, we assume that the energy consumption of a link uv is $\mathbf{c}(\|uv\|) = \|uv\|^2 + c$, where c is a constant depending on the maximum transmission rage. Here, c could be the receiving energy at v while $\|uv\|^2$ is the transmission energy. For example, for sensor nodes using 2.4 GHz IEEE 802.15.4 radio [2], the receiving energy is fixed as 18.8mA, while the transmission energy is from 8.5mA to 17.4mA. The values of η_1 and η_2 in LEARN routing are set as $1/2$ and 2.

Figure 6(a) and (d) illustrates the average delivery ratios of the five routing methods in 2D random networks and 3D random networks, respectively. Clearly, the delivery ratio increases when r increases. After r is larger than a certain value, it always guarantees the delivery. Notice that LEARN routing methods without using greedy routing as backup (denoted as LEARN) have lower delivery ratio under the same circumstance than classical greedy routing (denoted as Greedy), since they have smaller region to select the next hop node. With greedy backup, the delivery ratios of LEARN methods (denoted as LEARN-G) are almost the same with those of classical greedy routing.

The remaining figures in Figure 6 illustrate the average length stretch factors and energy stretch factors of all routing methods. Here, the *length/energy stretch factor* of a path from node s to node t is the ratio between the total length/energy of this path and the total length/energy of the optimal path connecting s and t. Smaller stretch factor of a routing method shows better path efficiency. For the length stretch factor, the LEARN methods with $\alpha = \pi/6$ has the best length efficiency. It is surprising that with $\alpha = \pi/4$ the length of LEARN path could be longer than simple greedy. However, when considering the energy efficiency, all LEARN methods can achieve better path efficiency than simple greedy method. Notice that smaller restricted region leads to better path efficiency, however it also has lower delivery ratio. Therefore, it is a trade-off between path efficiency and packet delivery. It is also clear that when the network is dense (with large transmission radius), LEARN and LEARN-G are almost the same, since LEARN can always find nodes inside the restricted region. Notice that LEARN often uses links that are shorter than the one used by greedy routing, and thus its routing path often has more hops than greedy. The disadvantage of more hops is compensated by generally the improved reliability of shorter links.

Besides deploying random networks in a rectangle or a cubic region, we also performed simulations for networks deployed in a disk or a spherical region. The conclusions from these simulations are consistent with the simulations for random network deployed in rectangle or a cubic region. Finally, in the conference version of this paper [3], routing performance of our LEARN routing in mobile networks can be founded. Due to the space limit, we ignore them here.

REFERENCES

[1] P.-J. Wan, C.-W. Yi, L. Wang, F. Yao, and X. Jia, "Asymptotic critical transmission radius for greedy forward routing in wireless ad hoc networks," *IEEE Tranc. of Parallel and Distributed Systems*, Vol. 57, No. 5, pp. 1433-1443, 2009. Short version in *ACM MobiHoc*, 2006.

[2] Datasheet, "2.4 GHz IEEE 802.15.4 / ZigBee-ready RF Transceiver (Rev. B)", Texas Instruments, 2007.

[3] Y. Wang, W.-Z. Song, W. Wang, X.-Y. Li, and T.A. Dahlberg, "LEARN:Localized Energy Aware Restricted Neighborhood Routing for Ad Hoc Networks," in *Proc. of IEEE SECON*, 2006.